



# Void swelling and irradiation creep of two high-nickel steels after irradiation at 400–410°C to 84–91 dpa in the BN-350 fast reactor

S.I. Porollo<sup>a</sup>, A.M. Dvoriashin<sup>a</sup>, A.N. Vorobjev<sup>a</sup>, Yu.V. Konobeev<sup>a</sup>,  
V.M. Krigan<sup>a</sup>, E.G. Mironova<sup>b</sup>, N.I. Budykin<sup>b</sup>, F.A. Garner<sup>c,\*</sup>

<sup>a</sup> Institute of Physics and Power Engineering, Obninsk, Russian Federation

<sup>b</sup> Bochvar's Research Institute of Nonorganic Materials, Moscow, Russian Federation

<sup>c</sup> Materials Resources Department, Pacific Northwest National Laboratory, 902 Battelle Boulevard, P8-15 Richland, WA 99352, USA

## Abstract

The relationship between irradiation creep and void swelling has been extensively studied for 300 series stainless steels with relatively low-nickel content. Similar studies on high-nickel alloys are not so common, however. An experiment conducted at  $\sim 400^\circ\text{C}$  and 84–91 dpa on two Russian high-nickel steels in the BN-350 fast reactor demonstrates that the form of the creep law and the creep–swelling relationship are not changed significantly at higher nickel levels. © 2000 Elsevier Science B.V. All rights reserved.

## 1. Introduction

The absence of a neutron source with fully fusion-relevant neutron spectra requires that experimental studies must use surrogate irradiation facilities, which in most cases must be conducted for long times in fast reactors in order to reach the required neutron fluences. Such irradiations of necessity focus on only a few alloys at a time and it is always valuable to look for generalized swelling–creep relationships that can be applied to a wider range of alloys and irradiation spectra.

Neutron-induced irradiation creep in low-nickel austenitic alloys and its relationship to void swelling has been a heavily researched subject, with most high-fluence data generated in fast reactors on 300 series stainless steels. As reviewed by Garner [1], all commonly used austenitic alloys exhibit essentially identical creep behavior where the creep compliance in the absence of swelling, designated  $B_0$ , is relatively independent of composition, thermal-mechanical starting state and

irradiation temperature. It was later realized by Garner and co-workers [2,3] that this independence also applied to the atomic displacement rate and the helium/dpa ratio. In the presence of void swelling, however, the creep rate increases directly with swelling rate such that all parametric dependencies of the creep rate directly reflect the dependencies of swelling [1]. The creep compliance  $B_0$  is of the order of  $\sim 1 \times 10^{-6} \text{ MPa}^{-1} \text{ dpa}^{-1}$  and the creep–swelling coupling coefficient  $D$  is initially  $0.6\text{--}1.0 \times 10^{-2} \text{ MPa}^{-1}$ , but declines as the swelling rate increases.

Recent studies by Toloczko and Garner have shown that this creep model can be extended to ferritic/martensitic alloys [4,5] and to austenitic alloys with higher nickel content [6]. Studies conducted by the authors of this paper have also shown that creep of low-nickel stainless steels used in Russia also conform to this model [7,8].

To this time, however, there are insufficient data available to determine whether these values of creep coefficients also apply to gamma-prime strengthened nickel-base alloys as well, especially in alloys that are more resistant to swelling than most 300 series austenitic steels. This paper explores the swelling–creep relationship of two high-nickel Russian steels with very different

\* Corresponding author. Tel.: +1-509 376 4136; fax: +1-509 376 0418.

E-mail address: frank.garner@pnl.gov (F.A. Garner).

swelling behavior. These are a solute-modified version of EP-753, and precipitation-hardened ER-16, similar to the Western alloy designated Nimonic PE-16. Both alloys are based on the Fe–(16–18)Cr–40Ni–(Ti–Al–Nb) alloy system. EP-753 (18Cr–40Ni–5Mo–Mn–Nb) normally has no gamma-prime phase but Ti and Al additions were made to develop such precipitates. The chemical compositions of the two alloys are shown in Table 1.

## 2. Materials and test methods

Thin-walled tube specimens were fabricated from experimental melts of the EP-753–Ti–Al and ER-16 alloys. The design of these tubes is shown in Fig. 1 and is identical to tubes used in studies on low-nickel alloys [7,8]. The ER-16 alloy was prepared by melting in air in an inductance furnace, followed by arc-re-melting in vacuum. After fabrication the ER-16 tubes were solution annealed at 980°C for 10 s using an electrical resistance method. The EP-753–Ti–Al alloy was prepared by vacuum melting in an inductance furnace followed by re-melting in vacuum. These tubes were solution annealed at 1020°C for 5 min and then 20% cold worked.

The tubes were pressurized with argon and the gas pressure was controlled by a manometer to produce hoop stresses in the range 0–300 MPa at the irradiation temperature. Before irradiation, the outer diameters of the tubes were measured by a micrometer with an error of  $\pm 0.005$  mm in the two perpendicular directions at three cross-sections along the tube axis. The results of 12 measurements were averaged for each creep tube. One stress-free tube was included along with two tubes each at hoop stress levels of 75, 150 and 300 MPa.

The specimens were irradiated in a special fueled subassembly, in which several central pins were replaced by a removable container. All tubes of a given alloy were irradiated side-by-side in perforated stainless steel baskets allowing for contact with flowing sodium coolant. The subassembly was loaded into the fourth row of the low enrichment zone of the BN-350 reactor in Kazakhstan. The total exposure time during eight runs was 631 effective days, reaching an irradiation dose of 91 dpa (NRT) for the ER-16 alloy and 84 dpa for the EP-753–Ti–Al alloy at the axial center of the creep tubes. The irradiation temperatures of 400°C for the ER-16 alloy and 410°C for the EP-753–Ti–Al alloy were dependent on the axial location of baskets. These temperatures were calculated from knowledge of the heating rates and sodium coolant flow rates, with an assessed accuracy of  $\pm 10^\circ\text{C}$ .

After removal from the reactor, the tubes were examined visually using an optical device at 10-fold magnification to search for flaws developed during irradiation. The specimens were then cleaned in ethyl

Table 1  
Chemical composition and treatment of alloys investigated

Alloy	Content (wt%)										Heat treatment
	C	Mn	Si	S	Cr	Ni	Mo	Nb	Ti	Al	
1 ER-16	0.053	1.72	0.17	0.005	16.10	40.10	3.91	0.53	0.92	1.15	Austenization at 1000°C for 30 min, solution treatment at 980°C for 10 s.
2 EP-753–Ti–Al	0.017	1.73	0.07	0.009	18.18	39.70	5.34	0.48	1.12	0.63	Austenization at 1000°C for 20 min, solution treatment at 1020°C for 5 min + 20% CW.

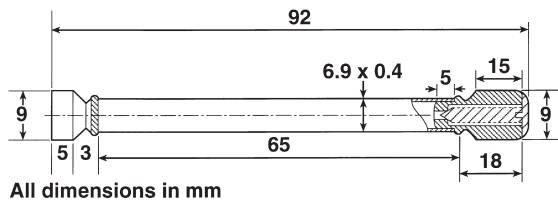


Fig. 1. Creep tube design.

alcohol to remove sodium oxides and then lightly polished with abrasive paper. The outer diameters of specimens were measured by an electrically driven micrometer with an error of  $\pm 0.005$  mm. The central 50 mm of the tubes was then measured in two perpendicular directions for three cross-sections along the tube length. The diameter changes measured for these cross-sections were averaged.

The tubes were then punctured in a vacuum chamber located in a hot cell to provide a measurement of the internal pressure at the end of the experiment. The measurement accuracy of the volume of gas released is 0.3–1.0 cm<sup>3</sup>. When a pressure loss is detected, however, it can not be directly determined whether depressurization occurred during irradiation or during removal and handling.

Subsequently, a section 50 mm in length was cut from the center of the tubes. The swelling of these sections was deduced from the densities of non-irradiated and irradiated specimens, with measurements made by weighing in CCl<sub>4</sub>. The error of density measurements was less than 0.5%. The swelling levels reported are the mean values of six measurements, made three times each on the two specimens at each stress level. The creep strains were calculated by subtracting one-third of the measured swelling from the total diametral strain, assuming isotropic swelling.

### 3. Experimental results

No obvious defects were detected on the tube surfaces after irradiation. The dependence of total diametral strain, swelling and creep strain on stress in the ER-16 and EP-753–Ti–Al alloys is shown in Figs. 2 and 3, respectively.

As deduced from puncturing and gas volume measurements, however, all tubes of the ER-16 alloy were found to have lost pressure. As seen in Fig. 2, the tube diametral strains increase linearly with increasing hoop stress, increasing from 1.7% to 6.4% over the range 0–300 MPa. The dependence of swelling-induced strain on stress is not so pronounced, however, ranging only from 1.8% to 2.5%, calculated as one-third of the measured density changes of 5.4–7.5%.

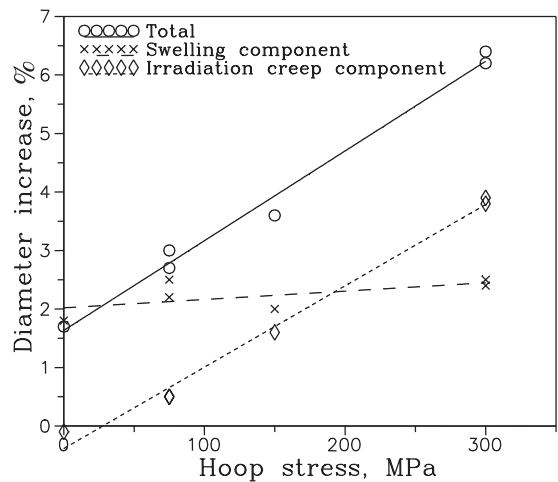


Fig. 2. The stress dependence of diametral strain, swelling and irradiation creep in the ER-16 alloy irradiated at 400°C to 91 dpa in the BN-350 fast reactor. Swelling strains are calculated as one-third of the measured density change. Negative creep strains imply some densification has occurred.

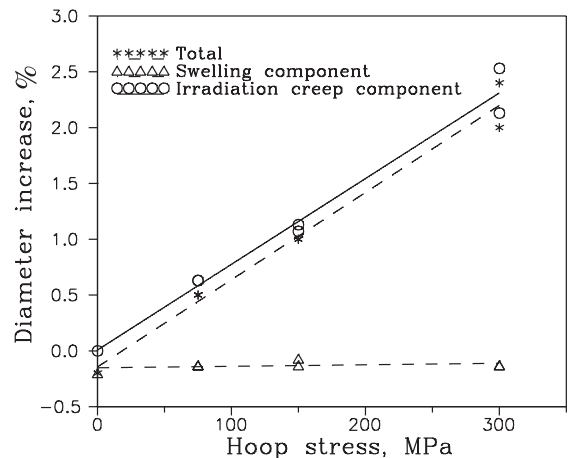


Fig. 3. The stress dependence of diametral strain, swelling and irradiation creep in the EP-753–Ti–Al alloy irradiated at 410°C to 84 dpa in the BN-350 fast reactor. Negative swelling strains imply some densification has occurred.

Of the six pressurized tubes of EP-753–Ti–Al both tubes at 150 MPa were found to have retained their pressure, but one tube with the starting stress of 75 MPa was found to have lost pressure. In the tubes, initially at 300 MPa, the measured hoop stresses appeared to be 6.8 and 9.3 MPa, indicating a near-total loss of pressure.

This alloy densified at all stress levels, indicating that swelling-induced strains were either zero or significantly less than the strains due to lattice parameter changes induced by segregation and precipitation. The diametral

strains increased with increasing stress level, ranging from 0% to 2.4% over the range 0–300 MPa.

#### 4. Discussion

Pressurized tubes that perform well under irradiation sometimes fail by development of microscopic holes in the weld region either during irradiation or more often after shutdown of the reactor and removal from the subassembly. In the former case, sodium coolant is often sucked back into the tube as the coolant temperature decreases. The absence of sodium in the tubes implies that the loss of pressure occurred after shutdown. The most frequently cited causes of such failure are thermal stresses and lowered ductility, both as a result of radiation hardening and physical injury during post-irradiation handling.

Even more importantly, the strains at 75 MPa in EP-753–Ti–Al are the same regardless of the difference in pressure, and all creep strains are strongly and linearly dependent on stress level. This strongly supports the assumption that pressure was lost after conclusion of the irradiation. It is considered highly unlikely that all tubes would have lost pressurization at the same time during irradiation.

The linear dependence of creep on stress level is consistent with most observations, as contained in Refs. [1–8].

The irradiation creep strain can be written in the following form [3]:

$$\frac{4}{3} \frac{\varepsilon_{\theta}}{\sigma_{\theta}} = \frac{\bar{\varepsilon}}{\bar{\sigma}} = BKt + DS^n, \quad (1)$$

where  $\bar{\varepsilon}$  and  $\bar{\sigma}$  are the effective strain and stress, respectively,  $Kt$  the irradiation dose in dpa,  $S$  the swelling and  $B$ ,  $D$  and  $n$  are the material parameters. In most recent studies,  $n = 1$ .

Since swelling in the EP-753–Ti–Al alloy does not exist under these irradiation conditions, Eq. (1) can be written as follows:

$$\frac{\varepsilon_{\theta}}{\sigma_{\theta}} = 0.75BKt, \quad (2)$$

yielding  $B = 1.2 \times 10^{-6} \text{ MPa}^{-1} \text{ dpa}^{-1}$ , similar to the  $B_0$  value extracted from most low-nickel alloys.

With data on swelling in the ER-16 alloy at only one dpa level it is not possible to clearly separate the  $B_0$  and  $DS$  contributions to the creep strain. However, the combined creep coefficient  $B$  is  $2.3 \times 10^{-6} \text{ MPa}^{-1} \text{ dpa}^{-1}$ . If we assume that  $B_0$  is also  $1.2 \times 10^{-6} \text{ MPa}^{-1} \text{ dpa}^{-1}$ , then we can calculate that the  $D$  coefficient is  $\sim 0.2 \times 10^{-2} \text{ MPa}^{-1}$ . This is in reasonable agreement with the results of other studies that show that  $D$  falls into this range as swelling increases.

The stress dependence of swelling on the ER-16 alloy can be described with an often-used expression [9–11],

$$S = S_0(1 + P\sigma_h),$$

where  $S_0$  is the measured stress-free swelling (5.4%),  $\sigma_h$  the hydrostatic component of stress and  $P$  is the swelling modulus. The value of  $P$  derived from the measured swelling values is  $2.6 \times 10^{-3} \text{ MPa}^{-1}$  for the ER-16 alloy. Using this value of  $P$  one can estimate a value of  $B_0$  of  $1.8 \times 10^{-6} \text{ MPa}^{-1} \text{ dpa}^{-1}$  for the ER-16 alloy. These values of irradiation creep and swelling moduli are in agreement with those of low-nickel alloys.

#### 5. Conclusions

It appears that the irradiation creep model and the creep–swelling relationship developed from experimental studies on low-nickel alloys also applies to high-nickel alloys. This allows the development of generalized creep equations for alloys not tested as extensively, provided that some data on the stress dependence of swelling can be obtained.

#### Acknowledgements

This work was supported in Russia by the Civilian Research and Development Foundation under Grants RE2-123 and GAP RPO-659, and in the US by the Office of Fusion Energy, US Department of Energy under Contract DE-AC06-76RLO 1830.

#### References

- [1] F.A. Garner, in: *Materials Science and Technology: A Comprehensive Treatment*, vol. 10A, VCH, 1994, p. 419 (Chapter 6).
- [2] F.A. Garner, M.B. Toloczko, *J. Nucl. Mater.* 251 (1997) 252.
- [3] F.A. Garner, M.B. Toloczko, M.L. Grossbeck, *J. Nucl. Mater.* 258–263 (1998) 1718.
- [4] M.B. Toloczko, F.A. Garner, in: R.K. Nanstad, M. Hamilton, F.A. Garner, A.S. Kumar (Eds.), *18th International Symposium on Effects of Radiation on Materials*, American Society of Testing and Materials, 1999, p. 765.
- [5] M.B. Toloczko, F.A. Garner, *J. Nucl. Mater.* 233–237 (1996) 289.
- [6] M.B. Toloczko, F.A. Garner, J. Standring, B. Munro, S. Adaway, *J. Nucl. Mater.* 258–263 (1998) 1606.
- [7] A.N. Vorobjev, N.I. Budylnkin, E.G. Mironova, S.I. Porollo, Yu.V. Konobeev, F.A. Garner, *J. Nucl. Mater.* 258–263 (1998) 1618.

- [8] S.I. Porollo, A.N. Vorobjev, Yu. V. Konobeev, N.I. Budylnin, E.G. Mironova, F.A. Garner, in: M.L. Hamilton, A.S. Kumar, S.T. Rosinski, M.L. Grossbeck (Eds.), ASTM STP 1366, 19th International Symposium on Effects of Radiation on Materials, American Society for Testing and Materials, Philadelphia, 1998, p. 679.
- [9] E.R. Gilbert, J.F. Bates, *J. Nucl. Mater.* 65 (1977) 204.
- [10] D.R. Harries, *J. Nucl. Mater.* 65 (1977) 157.
- [11] R.A. Weiner, J.P. Foster, A. Boltax, in: Proceedings of the International Conference on Radiation Effects in Breeder Reactor Structural Materials, Scottsdale, Arizona, 1977, pp. 865–878.